ISSN (Print) 1226-1750
ISSN (Online) 2233-6656
Journal of Magnetics 27(2), 172-178 (2022) https://doi.org/10.4283/JMAG.2022.27.2.172

Magnetic Properties and Microstructure of DyAlCu-diffusion Sintered Nd-Fe-B Magnets

Chunfa Liao[1,2]*, Xun Zhou[1,2], Peng Jiang[1,2], Zhiyong Zeng[1,2], and Lianghua Que[1,2]

[1]*Faculty of Materials Metallurgy and Chemistry, Jiangxi University of Science and Technology, Ganzhou 341000, China*
[2]*National Innovation Center for Rare Earth Functional Material, Jiangxi University of Science and Technology, Ganzhou 341000, China*

(Received 18 January 2022, Received in final form 25 March 2022, Accepted 8 April 2022)

The ability to improve the coercivity of sintered Nd-Fe-B diffused by Dy-Al-Cu alloy derived from electrolysis in a fluoride salt-oxide system was evaluated. The results show that with the increase in heat treatment time, the coercivity of the magnet firstly increased and then decreased. Holding at 900 °C for 4 h, tempering at low temperature for 3 h at 550 °C, the coercivity of GBDPed magnet increased by 44.34 %, the remanence decreased by 1.26 %, the Dy-rich shell phase was recognizable, and the Nd-rich phase evenly distributed. Electron microscope analysis showed that when the GBDP time was longer than 4h, the diffusion of Dy from the shell phase to the matrix phase dominated, decreasing the coercivity with the increase in the diffusion time. The increase of Fe content in the grain boundary phase enhanced the exchange coupling between grains, which also reduced the coercivity of the GBDPed magnet. The infiltration of the matrix phase by excessive Dy and deterioration of (00L) texture of Nd-Fe-B resulted in the reduction of the remanence and the maximum energy product.

Keywords : Sintered Nd-Fe-B magnets, Molten salt electrolysis, Grain boundary diffusion, Heat treatment time, Coercivity

1. Introduction

In the 21st century, the strategic goal of "peak carbon dioxide emissions, carbon neutrality" has spurred the vigorous development of new energy energy-saving, and environmental protection categories such as new energy vehicles, energy-saving inverter air conditioners, wind power generation, energy-saving elevators and intelligent manufacturing. NdFeB permanent magnets are widely used in these fields because of their excellent magnetic properties, and the power saving rate of high-performance NdFeB motors is as high as 15 %-20 % [1]. Rare earth elements and their alloys are gradually becoming the first choice of additives for high-performance permanent magnet materials such as Dy and Tb. By grain boundary diffusion process (GDBP) can not only effectively improve the comprehensive magnetic properties of magnets but also greatly reduce the usage amount of heavy rare earth elements and improve the cost performance [2].

Compared with the doping method, powder metallurgy method, and metal thermal reduction method, the molten salt electrolysis method in the rare earth alloy preparation method has the advantages of convenient operation, continuous production, environmental friendliness, and strong controllability [3-5]. In recent years, Cu and Al are mainly added to improve the grain boundary microstructure in the production of Nd-Fe-B magnets [6]. The melting point of Dy-Al-Cu alloy is lower than that of Dy, Dy-Al, and Dy-Cu. The comparison shows the theoretical conditions for Dy-Al-Cu alloy to replace dysprosium and its alloy mentioned above. It can be concluded that Dy-Al-Cu alloy has great application potential as a new additive for preparing high-performance NdFeB permanent magnet materials.

Based on the above considerations, the low melting point Dy-Al-Cu ternary alloy prepared in a fluoride-oxide system is used as the grain boundary diffusion source, which infiltrates into commercial sintered NdFeB magnets to improve magnetic properties. By controlling different heat treatment times, the microstructure and magnetic properties of GBDPed magnets were studied. The morphology and chemical composition of the grain boundary region

*Corresponding author: Tel: +86-0797-8312332
Fax: +86-0797-8312332, e-mail: liaochfa@163.com

were characterized, and the diffusion behavior of Dy element in magnets was discussed, to clarify the influence mechanism of diffusion treatment on the magnetic properties of NdFeB sintered magnets.

2. Materials and Methods

The original magnet used in this experiment is a commercial sintered Nd-Fe-B magnet (Ganzhou FORTUNE Electronics Co., Ltd.), machined into a 10 mm × 10 mm × 5 mm cube. The Dy-Al-Cu alloy used as the diffusion source in the experiment was obtained from electrolysis at 950 ℃ for 4 hours at a constant current of 20 A in LiF-DyF_3-Dy_2O_3 (2 wt.%)-Cu_2O (1 wt.%) molten salt system, graphite anode, tungsten cathode, corundum crucible serves as a receiving crucible and provided Al element at the same time. ICP-MS (ICAP-6300) analysis shows that the composition of Dy-Al-Cu alloy is $Dy_{68}Al_{24}Cu_8$ (at.%). Then, the alloy ingot was placed in a high-vacuum single-roll rotary quenching device (Shenyang AutoVac Vacuum Technology Co., Ltd.), and the rotating speed of the copper roll was controlled to be about 10 m/s, and $Dy_{68}Al_{24}Cu_8$ alloy thin strip was obtained under argon protection, as shown in Fig. 1(b). The magnet and alloy strips were polished with sandpaper, put into a beaker containing alcohol, cleaned in an ultrasonic cleaner, and finally dried for standby. The upper and lower surfaces of the magnet were covered with an alloy strip to form a diffusion couple and placed in a ceramic crucible. The direction of diffusion into the magnet was parallel to the C axis of the magnet, as shown in Fig. 1(a). The ceramic crucible was put into a vacuum sintering furnace (HTO-150H), vacuumed to below 1.0×10^{-3} Pa, raised the temperature to 900 ℃ at a constant heating rate of 7.5 ℃/min, and kept the temperature for different GBDP times (1-8 h). After cooling to room temperature, the temperature was raised to 550 ℃ at a constant heating rate of 7.5 ℃/min, and then tempered for 3 hours to obtain GBDPed magnets.

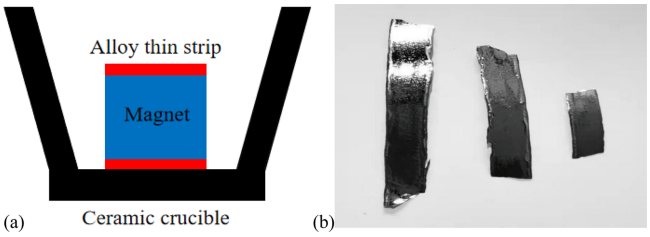

Fig. 1. (Color online) (a) A diffusion couple formed by covering a magnet with an alloy thin strip; (b) Alloy thin strip.

A high-temperature permanent magnet measuring instrument (NIM-500C) was used to analyze the magnetic properties of the magnet before and after treatment. The microstructure was characterized from a Zeiss scanning electron microscope (ΣIGMA). Energy-dispersive X-ray spectroscopy (EDS) was conducted to analyze the distribution of elements in the grain boundary region of the magnets before and after diffusion treatment. XRD analysis of the magnets before and after diffusion was performed from an X-ray diffractometer (Empyrean type). The melting point of $Dy_{68}Al_{24}Cu_8$ was determined from the analysis of the thermogravimetry-differential scanning calorimetry (TG-DSC) curve, which was measured from 25 ℃ to 1000 ℃ at the heating rate of 10 ℃/min.

3. Results and Discussion

3.1. Grain boundary diffusion source

$Dy_{68}Al_{24}Cu_8$ alloy was prepared by electrolysis in a fluoride salt-oxide system, and its alloy ribbon was obtained from a high vacuum single-roll rotary quenching equipment. After Dy infiltration, $(Nd, Dy)_2Fe_{14}B$ compound formed in the epitaxial layer of matrix phase grains of Nd-Fe-B magnet, which is of obvious core-shell structure

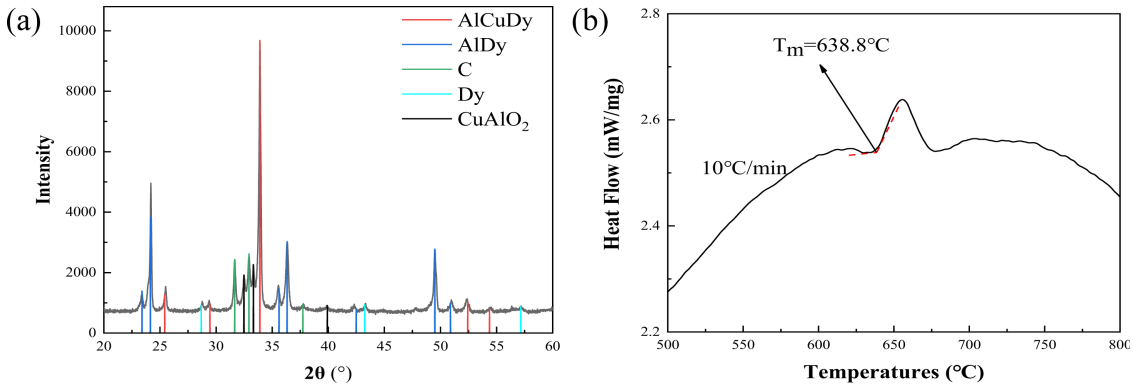

Fig. 2. (Color online) (a) XRD pattern of $Dy_{68}Al_{24}Cu_8$ alloy thin strip; (b) TG-DSC curve of $Dy_{68}Al_{24}Cu_8$ alloy strip heated to 1000 ℃ at room temperature by 10 ℃/min.

in microstructure, and the magnetocrystalline anisotropy of grains is enhanced, which greatly improves the coercivity of magnet. Both Al and Cu contribute to improving the wettability between the intergranular phase and matrix phase, enhancing the microstructure of the magnet, effectively weakening the magnetic exchange coupling between adjacent matrix phase grains, and strengthening the coercivity of the magnet. $Dy_{68}Al_{24}Cu_8$ is a eutectic alloy, which is composed of intermetallic compounds DyAlCu, DyAl, and solid solution β-Dy at room temperature. Fig. 2(a) shows the XRD pattern of the $Dy_{68}Al_{24}Cu_8$ alloy thin strip, the diffraction peaks corresponding to three phases (master alloys AlCuDy, AlDy, and solid solution β-Dy), the peaks of copper-aluminum oxide compounds, and few diffraction peaks of C are observed. The mass fraction of carbon in the alloy determined by the carbon/sulfur analyzer is 2.71×10^{-5}, which is due to the inevitable introduction of C impurity when graphite crucible was used as an electrolysis anode in molten salt electrolysis. According to the TG-DSC curve of the $Dy_{68}Al_{24}Cu_8$ alloy thin strip, the initial melting temperature of the alloy is 638.8 °C, as shown in Fig. 2(b).

3.2. Magnetic properties

The change in magnetic properties of the magnet with heat treatment times (1-8 h) at 900 °C and annealing at 550 °C for 3 hours as shown in Fig. 3(a). The demagnetization curves of the original magnet, the magnet without alloy only after heat treatment, and the magnet with alloy diffusion treatment are shown in Fig. 3(b), and the corresponding magnetism is summarized in Table 1.

As shown in Fig. 3(a), the coercivity of GBDPed magnets firstly increased and then decreased with the prolongation of the GDBP time. The highest coercivity was obtained for GBDPed magnets with the $Dy_{68}Al_{24}Cu_8$ alloy at 900 °C 4 h + 550 °C 3 h. The coercivity of the magnet only heat treated without $Dy_{68}Al_{24}Cu_8$ raised from 12.11 kOe to 12.62 kOe. As the GBDP time was 4 hours, the coercivity of the GBDPed magnet increased to 17.48 kOe from 12.11 kOe, and the corresponding remanence dropped from 14.23 kGs to 14.05 kGs. At the GBDP time of 8 hours, the coercivity of the GBDPed magnet rose to 16.75 kOe and the corresponding remanence decreased to 13.89 kGs. These results show that the increase of coercivity is caused by the GBDP with $Dy_{68}Al_{24}Cu_8$ alloy, rather than the changes caused by heat treatment. When the electrolytic alloy was used as a grain boundary diffusion source, a reasonable heat treatment time can ensure that the magnet obtains relatively high coercivity on the premise of almost without sacrificing remanence.

Figure 4 summarizes the reduction of remanence and the increase in coercivity for sintered NdFeB magnets treated with different Dy-based alloys and compared with the data in this study [7-11]. The electrolytic alloy contains a small amount of C impurity, which has a great influence on the coercivity [12]. Therefore, compared with other

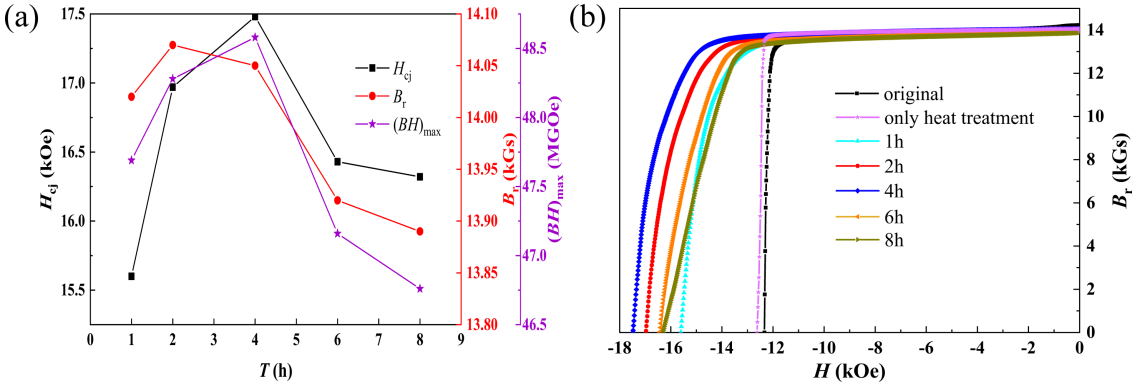

Fig. 3. (Color online) (a) Variation curve of magnetic properties of $Dy_{68}Al_{24}Cu_8$ GBDPed magnet with heat treatment time; (b) Demagnetization curve of $Dy_{68}Al_{24}Cu_8$ GBDPed magnet.

Table 1. The room temperature coercivity H_{cj}, remanence B_r and coercivity increasing range of the original magnet, the magnet only after heat treatment, and the magnet after diffusion treatment at 900 °C for 1 - 8 h + 550 °C for 3 h.

Sample	Original	Only heat treatment	1 h	2 h	4 h	6 h	8 h
B_r (kGs)	14.23	14.05	14.02	14.07	14.05	13.92	13.89
H_{cj} (kOe)	12.11	12.62	15.60	16.97	17.48	16.43	16.32
$\Delta H_{cj}/H_{cj}$ (%)	-	4.04	28.82	40.13	44.34	35.67	34.76
$\Delta B_r/B_r$ (%)	-	-1.26	-1.48	-1.12	-1.26	-2.18	-2.39

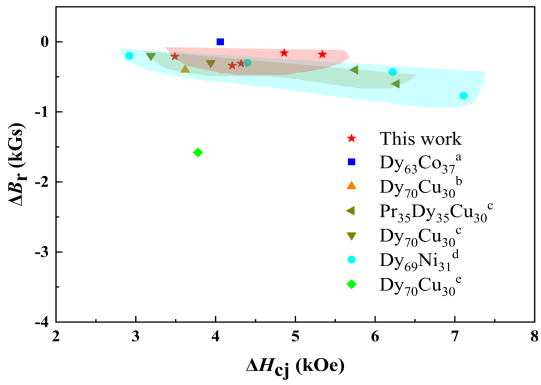

[a]Ref. [7], [b]Ref. [8], [c]Ref. [9], [d]Ref. [10], [e]Ref. [11].

Fig. 4. (Color online) Diagram of remanence decrease and coercivity increase sintered NdFeB magnets with different Dy-based alloys diffusion.

sintered Nd-Fe-B magnets with Dy-based alloys prepared by doping smelting as the diffusion source, the $Dy_{68}Al_{24}Cu_8$ alloy is beneficial to Nd-Fe-B magnet with high remanence.

According to the analysis in Fig. 3 and Table 1, with the extension of diffusion holding time, the decreased degree of remanence of GBDPed magnet increased, and the increase of coercivity first increased and then decreased. We deduce that the possible reason is that the main phase of the alloy obtained by electrolysis of a fluorine salt oxide system is a single AlCuDy phase, as shown in Fig. 2(a), $Dy_{68}Al_{24}Cu_8$ alloy has a fast diffusion rate. For the GBDP of sintered NdFeB, the diffusion of Dy in the c-axis direction of the magnet is limited [2]. With the extension of the GBDP time, changes in the microstructure of magnets and the diffusion path of Dy occur in the diffusion region. To understand the change of microstructure of diffusion surface of magnet with the GBDP time, the Dy-rich shell phase and intercrystalline phase of GBDPed magnet were deeply studied.

3.3. Microstructure

Both Fig. 5(a) and Fig. 5(b) exhibit the typical microstructure of Dy-free sintered NdFeB magnet, NdFeB matrix phase grains were in close contact with each other, which indicates that there was a phenomenon of magnetic exchange coupling between matrix phase grains. Different Fig. 5(a), the Nd-rich phase in Fig. 5(b) further concentrated, and the triple junction region increased. On the one hand, part of the Nd-rich phase formed some thin and continuous grain boundary phases between the grains of the matrix phase to eliminate the magnetic exchange coupling between the grains of the matrix phase and improve the coercivity of the magnet. Alternatively, some Nd-rich phases enriched in the intergranular triple junction

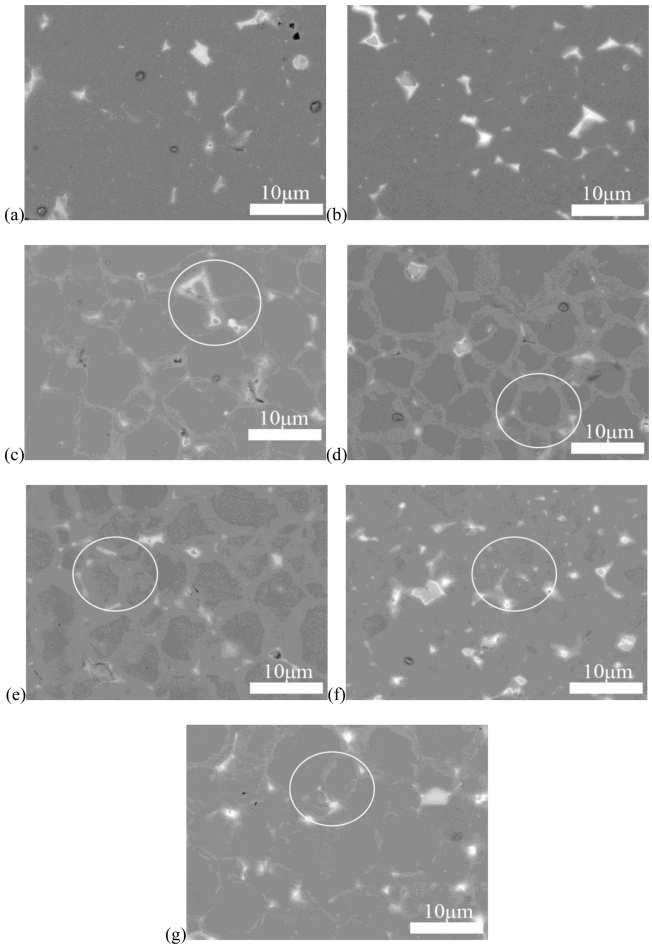

Fig. 5. SEM images of sintered NdFeB magnets about 100 microns from the diffusion surface before and after diffusion. (a) Original magnet; (b) Only heart treated magnet; (c) Diffusing magnet at 900 °C - 1 h + 550 °C - 3 h; (d) Diffusing magnet at 900 °C - 2 h + 550 °C - 3 h; (e) Diffusing magnet at 900 °C - 4 h + 550 °C - 3 h; (f) Diffusing magnet at 900 °C - 6 h + 550 °C - 3 h; (g) Diffusing magnet at 900 °C - 8 h + 550 °C - 3 h.

region generated a local demagnetization field, which reduced the coercivity of the magnet. The improvement in coercivity offset the weakening of magnetic exchange coupling between matrix phase grains and the effect of local demagnetization. The SEM images of the GBDPed magnet display typical core-shell structures of heavy rare earth grain boundary diffusion treated magnets, as shown in Fig. 5(c)-(g). Comparing Fig. 5(c) and Fig. 5(e), the grain boundary phase of the magnet diffused at 900 °C - 4 h + 550 °C - 3 h was thicker and the thickness of the Dy-rich shell phase increased, but the contrast between Dy-rich shell phases was weaker. We surmise that caused by the existence of intergranular magnetic exchange coupling between Dy-rich shell phases [12], and with the extension of the GBDP time, it tended to increase. Observed from

Fig. 5(c)-(e), the thickness of the Dy-rich shell phase increased with the extension of the GBDP time. As a result, the magnetic anisotropy increased, corresponding to the coercivity increased with the prolongation of heat treatment time. The boundary between the Nd-rich phase and the main phase was clear, and the grain of the matrix phase became round, indicating that the wettability of the grain boundary phase was improved. The Nd-rich phase further gathers in the triple junction region, mainly composed of Nd-rich oxide [11]. The local demagnetization field may be produced by the massive enrichment of Nd-rich oxides [14], and Nd of Nd-rich oxides originates from the layered grain boundary phase between Nd-Fe-B grains [12]. Fig. 5(f) and Fig. 5(g) show that the Nd-rich phases appeared inside the matrix phase, which destroyed the magnetic domain arrangement of the matrix phase, reducing coercivity [15].

To thoroughly analyze and find the reason for the decrease of coercivity with the GBDP time, the variation of the concentration distribution of Dy during GBDP with the GBDP time was quantitatively investigated. In the circular regions selected in Fig. 5, we chose three points from the grain boundary phase, shell phase, and matrix phase, respectively. The average value of each sample was calculated, as shown in Fig. 6. The Dy content in the matrix phase increased slowly within 1-4 hours and increased significantly after 4 hours. The core-shell structure with high Dy content in the shell phase and low Dy content in the matrix phase is beneficial to improve the coercivity [16]. The Dy content in the Dy-rich shell phase peaked at 4 h and then decreased with an increase in the GBDP time. Therefore, as the GBDP time increased, the

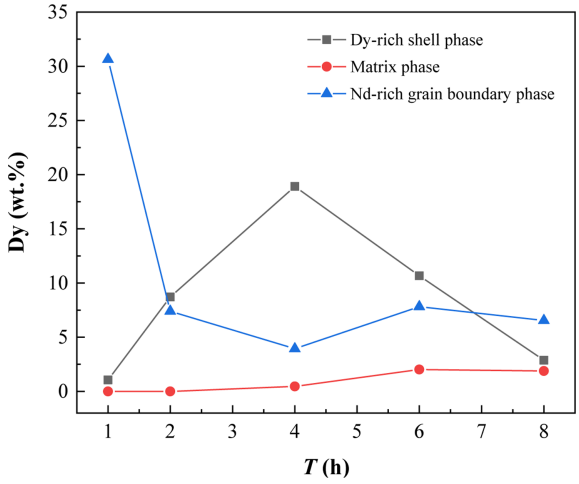

Fig. 6. (Color online) Average Dy content after GBDP for diffusion time.

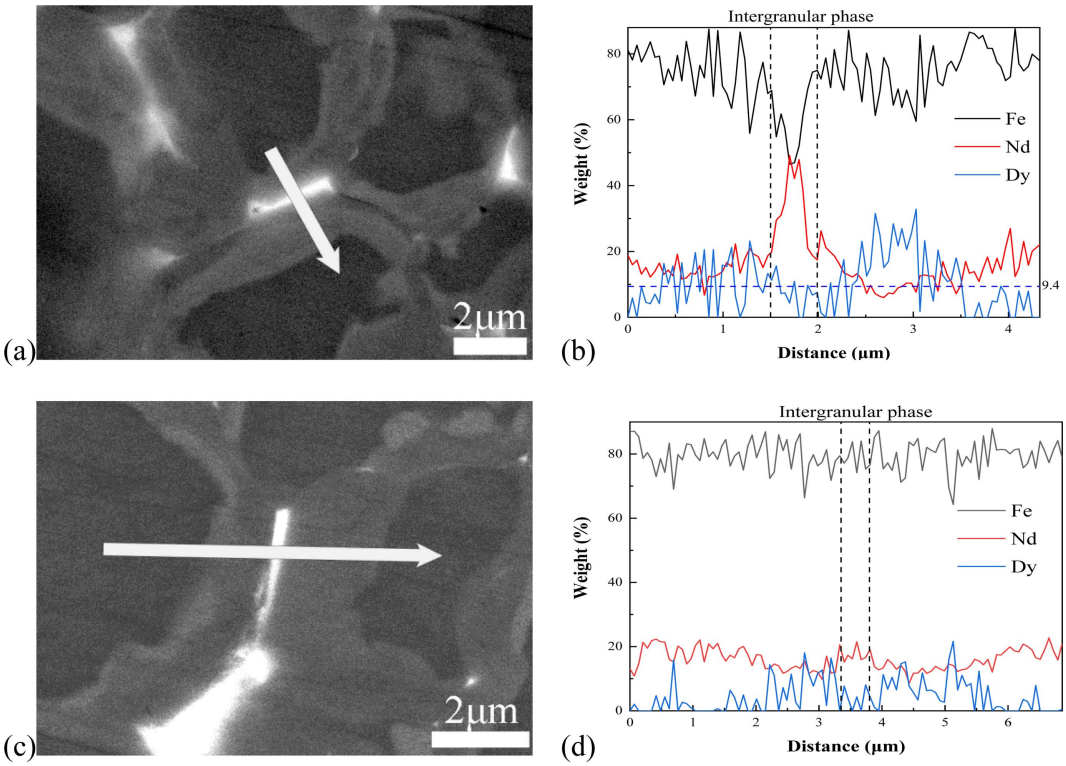

Fig. 7. (Color online) SEM images (100 microns from the diffusion surface) of Dy-rich shell phase and grain boundary phase of the GBDPed magnets with different heat treatment time, and EDS composition distribution of the lines shown. (a) and (c) 900 °C - 4 h + 550 °C - 3 h; (b) and (d) 900 °C - 8 h + 550 °C - 3 h.

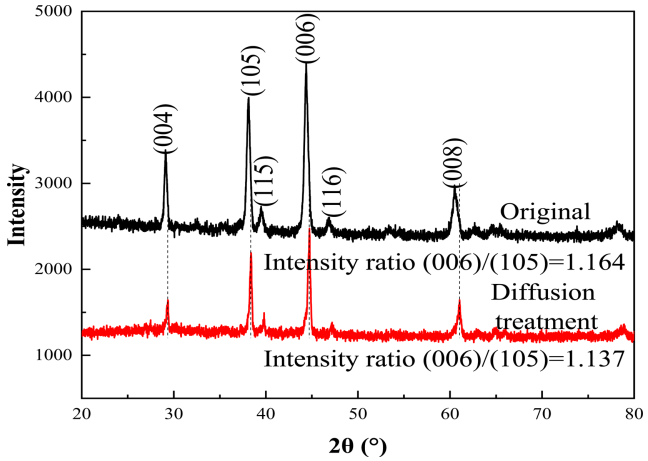

Fig. 8. (Color online) XRD diagram of diffusion surface of magnet before and after diffusion treatment.

coercivity of the GBDPed magnet increased first and then decreased. When the GBDP time exceeded 4 h, excessive Dy diffused into the matrix phase, so that the remanence and the maximum energy product of the magnet decreased with the increase in the GBDP time.

To further characterize the composition change of Dy in shell phase and intercrystalline phase after grain boundary diffusion, 900 ℃ - 4 h + 550 ℃ - 3 h and 900 ℃ - 8 h + 550 ℃ - 3 h diffusion treatment magnets selected. Different from Fig. 7(c), Fig. 7(d) shows that as the heat treatment time increased to 8 h, Fe content was higher in the grain boundary phase of the GBDPed magnet, while Dy content was slightly lower in the Dy-rich shell phase. Meanwhile, Dy was observed in the matrix phase. Fig. 7 indicates that with the extension of heat treatment time, Dy and Fe contents of matrix phase, shell phase, and grain boundary phase in the diffused region changed obviously. In terms of melting point, the melting point of (Nd, Dy)$_2$Fe14B was between that of $Dy_2Fe_{14}B$ and $Nd_2Fe_{14}B$ [17]. The matrix phase epitaxial layer melted at 900 ℃ and mixed with the diffused Dy at the grain boundary within 4 hours, then solidified to form a new Dy-rich shell phase. The calculation of the Dy substitution energy showed that the substitution energy of Dy atom in $Nd_2Fe_{14}B$ phase is much lower than that in the Nd-rich phase [18]. Such research shows that Dy is easier to enter the matrix phase from the grain boundary. However, when the grain boundary diffusion time was 8 hours, the Fe content in the intergranular phase increased. The strong ferromagnetism intercrystalline phase causes relatively low coercivity [19].

3.4. XRD analysis of magnet before and after diffusion

As shown in Fig. 8, the main diffraction peaks of the measured magnet correspond to the main diffraction peaks of the 2 : 14 : 1 matrix phase. The peak intensity ratio of I (006) / I (105) can roughly evaluate the degree of (00L) texture. The remanence of the magnet is related to the peak intensity ratio of I (006) / I (105) [20, 21]. The value of I (006) / I (105) decreased from 1.164 to 1.137 after long-time diffusion, which is consistent with the significantly decreased remanence. We hold that there are two possible reasons: firstly, the introduction of Dy decreased the crystal texture of the matrix phase [22]; secondly, Al and Cu doping reduced the melting point of the Nd-rich grain boundary phase and increased the fluidity of the Nd-rich grain boundary phase, which may also be unfavorable to the (00L) texture of Nd-Fe-B [23]. Observed from Fig. 8 all X-ray diffraction peaks of the GBDPed magnet shifted to the right, as shown in dashed lines. The substitution of Dy atoms for Nd atoms in the GBDP led to the decrease of the lattice constant of the matrix phase, proving Dy atoms entered the matrix phase to replace Nd atoms.

4. Conclusions

The results show that $Dy_{68}Al_{24}Cu_8$ alloy prepared by electrolysis has been successfully applied to the preparation of high-performance sintered NdFeB, and the following conclusions were obtained :

(1) Further purification of the electrolytic alloy after removing C as a diffusion source would further improve the comprehensive magnetic properties of the GBDPed magnet.

(2) Further enrichment of the Nd-rich phase, the increase of Fe content in the intercrystalline phase, and diffusion of Dy from the shell phase to matrix phase decreased the coercivity. The infiltration of the matrix phase by excessive Dy and deterioration of (00L) texture of Nd-Fe-B resulted in the reduction of the remanence and the maximum energy product.

(3) The diffusion behavior of Dy would varied with the heat treatment time: within 4 hours of heat treatment, Dy mainly diffused into the magnet matrix phase through the melted grain boundary phase, and formed a Dy-rich shell phase with the melted epitaxial layer; heat treatment time is more than 4 hours, the diffusion of Dy from the shell phase to the NdFeB matrix phase dominated in the GBDP.

Acknowledgement

This work was funded by the National Natural Science Foundation of China (No. 51674126) and the Key R&D Foundation of Ganzhou-Documents of Ganzhou Science

and Technology Bureau[2019]60.

References

[1] Shen Lu, Economic Research Guide. 35 (2019).
[2] Liu Zhongwu and He Jiayi, Acta Metall. Sin. **57**, 1155 (2021).
[3] Wu Wenyuan, Rare-earth metallurgy, Chemical Industry Press, Beijing (2005) pp 198.
[4] A. A. Omel' chuk, Russ. J. Electrochem. **46**, 680 (2010).
[5] Derek J. Fray, JOM. **53**, 27 (2001).
[6] Shouzeng Zhou, Qingfei Dong, and Xuexu Gao, Sintered Nd-Fe-B rare earth permanent magnet materials and technology, Metallurgical Industry Press, Beijing (2021) pp 82.
[7] J. Fliegans, C. Rado, R. Soulas, L. Guetaz, O. Tosoni, N. M. Dempsey, and G. Delette, J. Magn. Magn. Mater. **520**, 167280 (2021).
[8] Minghui Tang, Xiaoqian Bao, Kechao Lu, Lu Sun, Jiheng Li, and Xuexu Gao, Scr. Mater. **117**, 60 (2016).
[9] Kechao Lu, Xiaoqian Bao, Minghui Tang, Lu Sun, Jiheng Li, and Xuexu Gao, J. Magn. Magn. Mater. **441**, 517 (2017).
[10] Xiaolian Liu, Xuejiao Wang, Liping Liang, Pei Zhang, Jiaying Jin, Yujing Zhang, Tianyu Ma, and Mi Yan, J. Magn. Magn. Mater. **370**, 76 (2014).
[11] Xiaolian Liu, Yujing Zhang, Pei Zhang, Tianyu Ma, Mi Yan, Lizhong Zhao, and Lingwei Li, J. Magn. Magn. Mater. **468**, 165260 (2019).
[12] Zou Ning, Zheng Ju-gen, Zou Xu-jie, Zou Yong-bo, and Zou Yu-qin, Met. Funct. Mater. **23**, 51 (2016).
[13] T.-H. Kim, T. T. Sasaki, T. Ohkubo, Y. Takada, A. Kato, Y. Kaneko, and K. Hono, Acta Mater. **172**, 139 (2019).
[14] Y. H. Hou, Y. L. Wang, Y. I. Huang, Y. Wang, S. Li, S. C. Ma, Z. W. Liu, D. C. Zeng, L. Z. Zhao, and Z. C. Zhong, Acta Mater. **115**, 385 (2016).
[15] Y. Shinba, T. J. Konno, K. Ishikawa, and K. Hiraga, J. Appl. Phys. **97**, 053504 (2005).
[16] H. Y. Liu, G. Wang, Y. Hong, and D. C. Zeng, Acta Metall. Sin. (Engl. Lett). **31**, 496 (2018).
[17] Marie-Aline Van Ende, In-Ho Jung, Yong-Hwan Kim, and Taek-Soo Kim, Green Chem. **17**, 2246 (2015).
[18] X. B. Liu and Z. Altounian, J. Appl. Phys. **111**, 07A701 (2012).
[19] L. Henderson Lewis, Y. Zhu, and D. O., J. Appl. Phys. **76**, 6235 (1994).
[20] Lihua Liu, H. Sepehri-Amin, T. Ohkubo, M. Yano, A. Kato, N. Sakuma, T. Shoji, and K. Hono, Scr. Mater. **129**, 44 (2017).
[21] Lihua Liu, H. Sepehri-Amin, T. Ohkubo, M. Yano, A. Kato, T. Shoji, and K. Hono, J. Alloys Compd. **666**, 432 (2016).
[22] N. J. Yu, M. X. Pan, P. Y. Zhang, and H. L. Ge, Journal of Magnetics. **18**, 235 (2013).
[23] Y. I. Lee, H. W. Chang, G. Y. Huang, C. W. Shih, and W. C. Chang, IEEE Trans. Magn. **53**, 1 (2017).